ISSN: 2277-3754
ISO 9001:2008 Certified
International Journal of Engineering and Innovative Technology (IJEIT)
Volume 5, Issue 2, August 2015

Performance of prestressed concrete beam with FRP tendons

Mohamed Husain[1], Khaled Fawzy[2], and Ahmed Nada[3]
Structural Engineering Department, zagazig University, zagazig, Egypt

Abstract- ***Aggressive atmosphere and ground water increases the risk of corrosion of embedded reinforcement in concrete. Fiber Reinforced Polymers (FRP) bars and cables have proven as good answer to the corrosion problem. However, the structural behavior of concrete prestressed with FRP tendons has not been fully explored. The purpose of this research work is to assess the effects of some structural parameters on the behavior of prestressed concrete bridges with FRP prestressing tendons. Three-dimensional nonlinear finite element method (3D-NL-FEM) is used. Different models of prestressed concrete bridge tensioned with FRP cables-subject to four-point load system have been modeled and structurally analyzed on a commercial finite element analysis (ANSYS, 2013). A parametric study was conducted to examine the effects of prestressing reinforcement ratio, concrete compressive strength, and level of initial prestressing on the behavior. Three types of FRP cables are used: carbon fiber (CFRP), aramid fiber (AFRP), and glass fiber (GFRP). All the studied parameters affect the strength capacity, ductility and failure modes of the FRP-prestressed beam models.***

Index **— Prestressed concrete, FRP tendons, carbon fiber, Flexural Response.**

I. INTRODUCTION

The design and construction of FRP- prestressed concrete structures require more research work necessary to build up experience on their behavior. The design rules for FRP-prestressed concrete have not been fully developed in the current design codes in comparison with steel prestressed concrete structures. To solve this problem, experimental and analytical researches on the prestressed concrete with FRP tendons have been going on to gain knowledge about its behavior under different loading conditions and different structural parameters. Many researches [1-9] have recommended more studies in this field to enhance design guide lines.

Nabil F. Grace (2003) [10] found that for double tee beam prestressed with bonded and unbonded carbon fiber tendons, the ultimate load and the cracking load were, respectively, approximately 5.3 and 1.4 times the service load. Also Nabil F. Grace (2008) [11] has investigated primarily addressed the flexural performance of three concrete box-beam bridge models reinforced with prestressed CFCC, focusing on the effects of using unbonded longitudinal post-tensioning. It is found that, a greater level of total prestressing force prolongs the development of cracking and reduces the number and size of cracks that develop under loading, a greater level of total prestressing force reduces the amount of residual deflection. Designed as over-reinforced sections, had a failure that was sudden, without significant warning prior to its failure, while members with greater total prestressing force could fail suddenly.

J.W. Schmidt & B. Täljsten (2009) [12] found that No sufficient mechanical anchor system has been made yet, despite worldwide efforts to find a competitive FRP tendon anchorage, Several wedge shapes and different materials have been used in order to solve the problem of too high principal stresses at the anchor front and It is seen that no FRP anchor is yet implementable in external post-tensioning applications, which means that further improvements are necessary in order to make FRP pre-stressing systems commercially compete able.

Nabil F. Grace (2010) [13] found that the level of transverse post-tensioning forces and the number of transverse diaphragms did not significantly affect the load-distribution behavior of the bridge model in the un cracked-deck-slab phase. However, significant improvement of the load-distribution behavior was observed in the cracked-deck-slab phase. Martin NOËL (2007) [15] found that maintaining a constant reinforcement ratio, the GFRP-reinforced slab G1 displayed a similar ultimate capacity but reduced serviceability compared with the steel-reinforced control slab. Mid span deflections and flexural crack widths were 3 and 4 times those of the control slab, respectively, the mode of failure was changed from a ductile flexural failure to a brittle shear failure due to the low stiffness of the GFRP reinforcement, the addition of prestressed CFRP tendons resulted in excellent serviceability performance regardless of the number of tendons added.

The main objective of this research is to study the effects of prestressing reinforcement ratio ρ, concrete compressive strength f_{cu}, and level of prestressing (as a percentage of ultimate tendon resistance) on the flexural behavior of FRP-prestressed concrete bridges with different types fibers, such as carbon fiber (CFRP), aramid fiber (AFRP), and glass fiber (GFRP).

II. NON LINEAR FINITE ELEMENT MODELING

Research methodology is nonlinear (3-D) finite element modeling of prestressed concrete samples with FRP Tendons has been formulated. The model was analyzed under static vertical loads and horizontal compression forces at edges whose results from tendons stressing. The elements were solid65 for concrete; this element has eight nodes with three degrees of freedom at each node – translations in the nodal x, y, and z direction, link8 for prestressing reinforcement, this

ISSN: 2277-3754
ISO 9001:2008 Certified
International Journal of Engineering and Innovative Technology (IJEIT)
Volume 5, Issue 2, August 2015

element is a 3D spar element and it has two nodes with three degrees of freedom – translations in the nodal x, y, and z directions and beam188 for ordinary reinforcement. Full bond between the tendons and concrete face is assumed. The tested model finite element meshing is shown in Fig. (2).

III. VERIFICATION OF THE NON LINEAR FINITE ELEMENT MODELING

To verify the nonlinear finite element modeling constructed by the use of the nonlinear finite element analysis program ANSYS in the analysis of four models identical to those tested experimentally by Martin Noel (2007) [15] and Nolan Domenico (1995) [16] are prepared and constructed by the use of this program, their results are compared to those obtained experimentally. The comparison between both the experimental and finite element results is considered the base in checking the validity of the finite element modeling.

This comparison was carried out through the failure load. Model 1 is a slab strip with cross section and length 600mm×300mm, and 5000 mm respectively, clear span in loading was 4500 mm, with shear span 1750 mm, the top mat and transverse bottom reinforcements were glass fiber bars (GFRP) 13 mm @150mm., top and bottom clear cover were kept 30mm, bottom longitudinal direction consist of 6 steel bars 15mm @ 100mm. Model 2 has the same properties of model 1 but bottom longitudinal reinforcement consist of 6 GFRP bars 16 mm @ 100mm. Model 3 is a T- Section beam with total depth 320 mm, width of flange 300 mm, thickness of flange 80 mm and thickness of web 100 mm. This model was also post-tensioned with 1 CFRP 15.2 mm tendon at a depth of 260 mm, clear span in loading was 2800 mm with shear span 1200 mm. Model 4 has the same properties of model 3 but with shear span 700 mm.

Deflections and load capacities (Δ_u and P_u respectively) of experimental models versus FE models with differences in percentage were shown at table (1), it is seen that the FEM models provided good predictions against the experimental data, including average errors of 7.3%, and 17.5% for the ultimate loads and the maximum deflection, respectively.

Table 1 Deflections and load capacities of experimental versus FEM

Difference %		FEM results		Experimental		Model
Defl.%	Load %	Δ_u mm	P_u kN	Δ_u mm	P_u kN	
9.6	7.3	193	154.7	176	167	Model 1
17.5	2.4	91	170	110	166	Model 2
0	1.05	28.4	96	28.4	95	Model 3
13.7	5.4	24.7	155	29	164	Model 4

IV. PARAMETRIC STUDY

In this numerical study all models were rectangular (600 mm × 300 mm) with span 5000 mm, All carbon tendons had ultimate strength f_{ult} equal 1860 Mpa with modulus of elasticity E equal 165 Gpa, All aramid tendons had ultimate strength equal 1860 Mpa with modulus of elasticity equal 70 Gpa, and all glass tendons had ultimate strength equal 1724 MPa with modulus of elasticity equal 50 Gpa according to (CAN/CSA-S806-02) [14] table 2.

Table 2 Tensile properties of prestressing tendons [14]

Mechanical properties	Prestressing Steel	AFRP Tendon	CFRP Tendon	GFRP Tendon
Yield Stress(MPa)	1034-1396	N/A	N/A	N/A
Tensile strength(MPa)	1379-1862	1200-2068	1650-2410	1379-1724
Elastic Modulus(GPa)	186-200	50-74	152-165	48-62
Yield Strain %	1.4-2.5	N/A	N/A	N/A
Rupture Strain%	More than 4	2-2.6	1-1.5	3-4.5
Density (Kg/m3)	7900	1250-1400	1500-1600	1250-2400

Fig.1 and table 3 show the test specimen details. The effect of prestressing reinforcement ratio ρ (corresponding to over, balanced and under reinforced conditions), concrete compressive strength f_{cu}, and level of prestressing P% on the flexural behavior of prestressed concrete bridges with fiber tendons are studied using ANSYS finite element program. Twenty nine specimens with different types of FRP cables were numerically analyzed.

The first studied parameter is the prestressing reinforcement ratio ρ, where three different values for different type of FRP. Firstly for CFRP models C1, C2, and C3 with ρ values of 0.63 %, 0.494 %, and 0.294 %, respectively. Secondly, for AFRP models A1, A2, A3, and A4 with ρ values of 0.63 %, 0.494 %, 0.293 %, and 0.19 %, respectively. Thirdly, for GFRP models G1, G2, G3, and G4 with ρ values of 0.63 %, 0.494 %, 0.293 %, and 0.19 %, respectively. The models have constant prestress level (P = ***70%*** of the strand strength) and concrete compressive strength $f_{cu\ equal}$ 35 MPa.

The second studied parameter is concrete compressive strength f_{cu}, where three different values for different type of FRP. Firstly for CFRP models C5, C6, C7 and C8 with f_{cu} values of 35, 45, 50 and 60 MPa, respectively. Secondly, for AFRP models 5, A6, A7 and A8 with f_{cu} values of 35, 45, 50 and 60, respectively. Thirdly, for GFRP models G5, G6, G7, and G8 with f_{cu} values of 35, 45, 50 and 60, respectively. The models have constant prestress level (P = 60% of the strand strength) and prestressing reinforcement ratio ρ equal 0.56%.

The third studied parameter is the prestress level P, where three different values for different type of FRP. Firstly for CFRP models C9, and C10 with P values of 60 and 50% respectively, the concrete compressive strength f_{cu} equal 35

ISSN: 2277-3754
ISO 9001:2008 Certified
International Journal of Engineering and Innovative Technology (IJEIT)
Volume 5, Issue 2, August 2015

MPa and ρ equal 0.63 %. Secondly, for AFRP models A9 and A10 with P values of 60 and 50% respectively and ρ equal 0.49 %. Thirdly, for GFRP models G9 and G10 with P values of % and 50% respectively, and ρ equal 0.49%. The models have constant concrete compressive strength f_{cu} = 35 MPa.

Table 3 Test specimen details

Spec.	f_{cu} MPa	F_{ult} MPa	E	ρ%	P%
C1	35	1860	165000	0.63	70
C2	35	1860	165000	0.494	70
C3	35	1860	165000	0.294	70
C5	35	1860	165000	0.56	60
C6	45	1860	165000	0.56	60
C7	50	1860	165000	0.56	60
C8	60	1860	165000	0.56	60
C9	35	1860	165000	0.63	60
C10	35	1860	165000	0.63	50
A1	35	1860	70000	0.63	70
A2	35	1860	70000	0.494	70
A3	35	1860	70000	0.293	70
A4	35	1860	70000	0.19	70
A5	35	1860	70000	0.56	60
A6	45	1860	70000	0.56	60
A7	50	1860	70000	0.56	60
A8	60	1860	70000	0.56	60
A9	35	1860	70000	0.49	60
A10	35	1860	70000	0.49	50
G1	35	1724	50000	0.63	70
G2	35	1724	50000	0.494	70
G3	35	1724	50000	0.26	70
G4	35	1724	50000	0.19	70
G5	35	1724	50000	0.56	60
G6	45	1724	50000	0.56	60
G7	50	1724	50000	0.56	60
G8	60	1724	50000	0.56	60
G9	35	1724	50000	0.49	60
G10	35	1724	50000	0.49	50

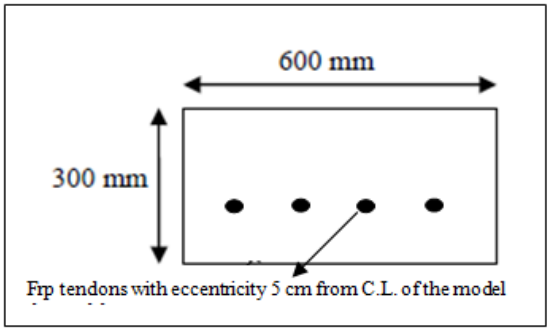

Fig: 1 Test specimen details.

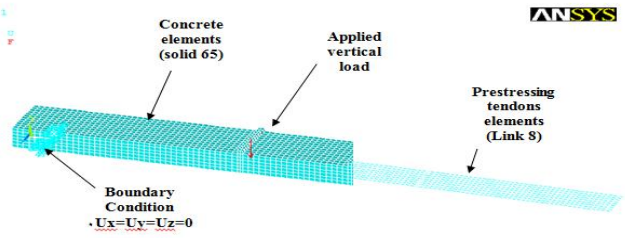

Fig: 2 Finite element models

V. RESULTS AND DISCUSSION

A. *Effect of prestressed reinforcement ratio (ρ)*

The results are shown in Table 4, Figure 3 and Figure 4 where (P_{cr} , Δ_{cr}), (P_{el} , Δ_{el}), and (P_u , Δ_u), which are the coordinates of first cracking point, elastic limit point (or yield), and ultimate point, respectively are given. Using information gained from load-deflection relations, the ductility index (μ_Δ), the over strength factor (Ω), the initial un-cracked elastic stiffness (K_i), the plastic stiffness (K_p) and the energy absorption index (E.A.I = the ratio of total area under load-deflection curve to area under elastic part at the same curve) are listed in Table 5. They are calculated from the following equations.

$\mu_\Delta = \Delta_u / \Delta_{el}$ ……. (1)
$\Omega = P_u / P_{el}$ ……. (2)
$K_i = P_{el} / \Delta_{el}$ ……. (3)
$K_p = (P_u - P_{el}) / (\Delta_u - \Delta_e)$ (4)

For the specimens CFRP (C1, C2, C3), the failure modes were brittle failure, and varied with changing prestressing reinforcement ratio (ρ). It can be observed by decreasing this ratio, failure mode changed from compression at concrete (C1) to tension at tendons (C3) Table 5. The over prestressing reinforcement ratio (ρ =0.63%) leads to significant improvement in flexural strength capacity with low ductility and deformability. The use of balanced prestressing reinforcement ratio (ρ =0.494%) leads to significant improvement in ductility, deformability and flexural strength capacity, the value of deformation capacity is almost increased by 50% by reducing prestressing reinforcement ratio from 0.633% to 0.494%, the over strength factor (Ω) is slightly increased with increasing the prestressing reinforcement ratios (ρ). The ductility index (μΔ) of the CFRP-prestressed beam with balanced (ρ) is found to be higher than that of CFRP-prestressed beam with compression (ρ) by about 20% and lower than that of CFRP-prestressed beam with tension (ρ) by about 24%. The energy absorption index (E.A.I) of C2 is found to be higher than that of C1 by about 40% and lower than that of C3 by about 25%.

For CFRP beams, with using of under prestressing reinforcement ratio (ρ =0.294%) leads to significant improvement in the ductility, deformability and low flexural capacity. Figure 4 show that, the increase of prestressed reinforcement ratios (ρ) for CFRP has increased the strength at the cracking and ultimate loads and also increased stiffness after cracking.

For the specimens AFRP (A1, A2, A3, A4), the failure modes are similar to o CFRP. It can be observed by decreasing the prestressing reinforcement ratio (ρ), the failure mode changed from compression (A1) to tension at tendons (A4). Using of over prestressing reinforcement ratio (ρ) leads to significant improvement in flexural capacity with low ductility and deformability until ρ%=0.494 which leads to good characteristics in ductility, deformability and flexural capacity. The value of deformation capacity of AFRP with (ρ %=0.494) is almost increased by 25% by reducing

ISSN: 2277-3754
ISO 9001:2008 Certified
International Journal of Engineering and Innovative Technology (IJEIT)
Volume 5, Issue 2, August 2015

prestressing reinforcement ratio from 0.633% to 0.494%. The ductility index (μ_Δ) of the AFRP-prestressed beam with (ρ =0.494%) is found to be higher than that of AFRP-prestressed beam with (ρ = 0.633%) by about 20%. The energy absorption index (E.A.I) of A2 is found to be higher than that of A1 by about 25%. Using of balanced prestressing reinforcement ratio leads to high ductility, deformability and low flexural capacity, while using of under prestressing reinforcement ratio leads to significant improvement in the ductility, deformability and low flexural capacity.

Similar to CFRP, the increase of prestressed reinforcement ratios (ρ) for AFRP has increased the strength at the cracking and ultimate loads and also increased stiffness after cracking. It may be noted, that the value of ultimate load decreased up to 50% by reducing prestressing reinforcement ratio (ρ) from 0.633 to 0.19%.

For the specimens GFRP (G1, G2, G3, G4), the failure modes were brittle failure, and varied with changing prestressing reinforcement ratio (ρ). It can be observed by decreasing this ratio, failure mode change from compression at concrete (G1) to tension at tendons (G4).Using of over prestressing reinforcement ratio (ρ) leads to significant improvement in flexural capacity with good ductility and deformability. Using of balanced prestressing reinforcement ratio (ρ) leads to high ductility, deformability and low flexural Capacity. Using of under prestressing reinforcement ratio (ρ) leads to significant improvement in the ductility, deformability and low flexural capacity.

The increase of prestressed reinforcement ratios (ρ) for GFRP has increased the strength at the cracking and ultimate loads and also increased stiffness after cracking. As the prestressing reinforcement ratio (ρ) decreased the value of ultimate load decreased. The deformation capacity of the GFRP-prestressed beam with ρ =0.633% is found to be higher than that of GFRP-prestressed beam with ρ = 0.494% by about 12%. The energy absorption index (E.A.I) and ductility index (μ_Δ) of the GFRP-prestressed beam with ρ =0.494% is found to be almost equal that of GFRP-prestressed beam with ρ =0.633 %.

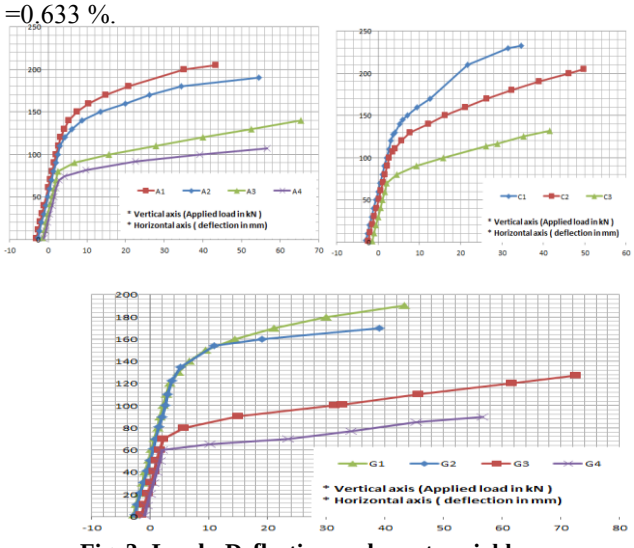

Fig. 3: Load - Deflections values at variable ρ

Table 4 Loads-Deflections values at variable ρ

Speci.	ρ%	P_{cr} kN	Δ_{cr} mm	P_{el} kN	Δ_{el} mm	P_u kN	Δ_u mm
C1	0.63	127.6	3.7	145	6	233	34.6
C2	0.494	107.2	3.5	130	7.7	208	53
C3	0.294	76	3.5	80	4.6	132	41.5
A1	0.63	128.4	3.8	140	5.3	205	43.2
A2	0.494	116	3.6	130	5.5	190	54.5
A3	0.293	80.7	3.5	93	4	140	65.3
A4	0.19	65	2.2	73	3.8	107	56.6
G1	0.63	122	3.4	140	6.6	190	43.4
G2	0.494	125	4	135	6	170	39
G3	0.26	75.4	4	81	5.7	127	72.6
G4	0.19	56	2	60	2.1	90	56.5

Table: 5 Computed structural characteristics for different ρ and cables

Speci.	ρ%	μ_Δ	Ω	K_i	K_p	K_p/K_i	E.A.I	Failure mode
C1	0.63	5.76	1.61	16111	3081	0.19	9.27	compression
C2	0.494	6.88	1.6	12871	1721	0.14	12.66	balanced
C3	0.294	9.02	1.65	13115	1409	0.11	17.03	tension
A1	0.63	8.15	1.46	16667	1715	0.1	12.12	compression
A2	0.494	9.91	1.46	15854	1224	0.08	15.71	compression
A3	0.293	16.3	1.51	16909	766	0.05	28.92	balanced
A4	0.19	14.9	1.47	14898	644	0.04	27.57	tension
G1	0.63	6.58	1.36	14737	1358	0.09	10.13	compression
G2	0.494	6.5	1.26	15698	1060	0.07	9.67	compression
G3	0.26	12.7	1.57	11408	687	0.06	25.2	balanced
G4	0.19	26.9	1.5	19355	551	0.03	44.87	tension

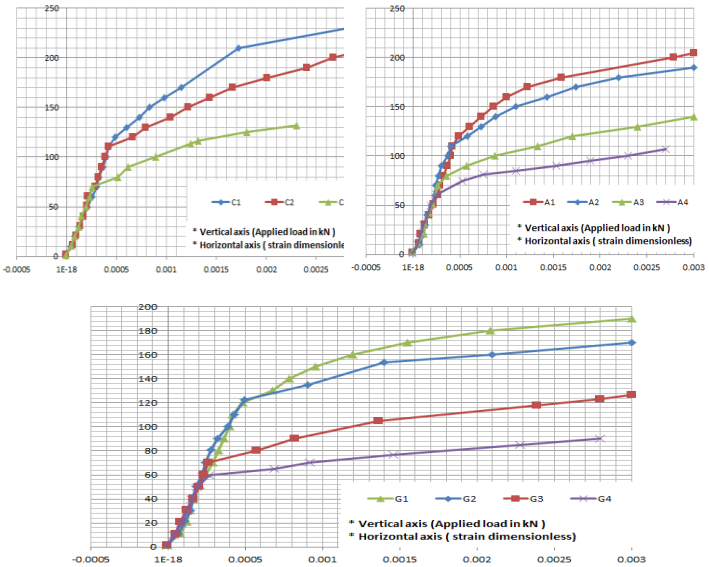

Fig: 4 Load-concrete strain relations

ISSN: 2277-3754
ISO 9001:2008 Certified
International Journal of Engineering and Innovative Technology (IJEIT)
Volume 5, Issue 2, August 2015

B. Effect of Concrete Compressive Strength (f_{cu})

To study the effect of concrete compressive strength (f_{cu}) on flexural response, twelve specimens prestressed with three types of FRP tendons, CFRP, AFRP, and GFRP, with different concrete compressive strengths were numerically analyzed. The results are shown in Table 6, Figure 5 and Figure 6 where (P_{cr} , Δ_{cr}), (P_{el} , Δ_{el}), and (P_u , Δ_u), which are the coordinates of first cracking point, elastic limit point (or yield), and ultimate point, respectively are given. Using information gained from load-deflection relations, the ductility index (μ_Δ), the over strength factor (Ω), the initial un-cracked elastic stiffness (K_i), the plastic stiffness (K_p) and the energy absorption index (E.A.I = the ratio of total area under load-deflection curve to area under elastic part at the same curve) are listed in Table 7.

For the specimens CFRP (C5, C6, C7, C8), the failure mode for these specimens is brittle failure, and be different at location with changing concrete compressive strength. Failure location is changed from compression zone at concrete to tension zone at tendons by increasing concrete compressive strength. Using of concrete compressive strength with 35 Mpa leads to significant improvement in the ductility, deformability and low flexural capacity. As the concrete strength for CFRP prestressed concrete increased, the μ_Δ and E.A.I decreased. Using of high concrete compressive strength with (50-60 Mpa) leads to slightly improvement in flexural capacity with deceasing in ductility index μ_Δ and E.A.I by about 25% and 15% respectively. It may be seen that, using of concrete compressive strength with 45 Mpa leads to best characteristics in both flexural capacity and serviceability stages.

For the specimens AFRP (A5, A6, A7, A8), the failure mode was brittle similar to the specimens of CFRP and its location was changed from compression zone at concrete to tension zone at tendons by increasing concrete compressive strength. The use of concrete compressive strength (35-45) MPa leads to low ductility, deformability and flexural capacity. Using of high concrete compressive strength (50-60) MPa leads to significant improvement in flexural capacity, ductility and deformability.

As the concrete strength increased, the deformation capacity of AFRP- prestressed beam as well as its ultimate load capacity is increased. The ductility index of the AFRP-prestressed beam with f_{cu}=60MPa is found to be higher than that of AFRP-prestressed beam with f_{cu}=35MPa by about 50%. The energy absorption index E.A.I of the AFRP-prestressed beam with f_{cu}=60MPa is found to be higher than that of AFRP-prestressed beam with f_{cu}=35MPa by about 80%. The plastic stiffness of the AFRP-prestressed beam with f_{cu}=60 MPa is found to be higher than that of AFRP-prestressed beam with f_{cu}=35MPa by about 45%. It may be seen that μ_Δ and E.A.I increases with an increase in concrete strength for AFRP prestressed concrete.

For the specimens GFRP (G5, G6, G7, G8), the failure mode is similar to the specimens of AFRP. Using of high concrete compressive strength (50-60) Mpa leads to significant improvement in flexural capacity, ductility and deformability. Using of concrete compressive strength (35-45) Mpa leads to low ductility, deformability and flexural capacity. As the concrete strength increased, the deformation capacity of GFRP- prestressed beam as well as its ultimate load capacity is increased. The values of deformation capacity and energy absorption index E.A.I are almost twice by reducing increasing f_{cu} from 35MPa to 60MPa. The ductility index of the GFRP-prestressed beam with f_{cu}=60MPa is found to be higher than that of GFRP-prestressed beam with f_{cu}=35MPa by about 85%. The plastic stiffness of the GFRP-prestressed beam with f_{cu}=60MPa is found to be less than that of AFRP-prestressed beam with f_{cu}=35MPa by about 30%.

Table 6 Loads-Deflections values at variable f_{cu}

Speci.	f_{cu} Mpa	P_{cr} kN	Δ_{cr} mm	P_{el} kN	Δ_{el} mm	P_u kN	Δ_u mm
C5	35	107	3.4	117	5	209	48.5
C6	45	112	3.3	130	6.2	235	60.5
C7	50	113.6	2.9	140	8.2	245	61
C8	60	118.4	3.3	145	8.7	250	62.4
A5	35	105.6	3.5	116	6	180	49
A6	45	110	3.5	120	5.3	200	58.5
A7	50	112	3.4	120	4.7	210	59.8
A8	60	117.6	3.9	125	5	245	61
G5	35	100.4	3	110	5	170	49.1
G6	45	110.8	3.2	120	4.5	185	60.6
G7	50	115	3.4	125	5	195	87
G8	60	110	3.6	120	5.6	210	99

Table 7 Computed data at variable f_{cu}

Speci.	μ_Δ	Ω	K_i	K_p	K_p/K_i	E.A.I	Failure mode
C5	9.7	1.78	15811	2106	0.13	17.36	compression
C6	9.76	1.8	15663	1933	0.12	19.37	compression
C7	7.44	1.75	13725	1988	0.14	15.24	tension
C8	7.17	1.72	13679	1955	0.14	14.8	tension
A5	8.17	1.55	13810	1488	0.1	14.06	compression
A6	11.04	1.67	16216	1503	0.09	20.17	compression
A7	12.72	1.75	17910	1633	0.09	23.61	compression
A8	12.2	1.96	18382	2142	0.12	25.38	compression
G5	9.82	1.55	15278	1360	0.09	16.59	compression
G6	13.47	1.54	17910	1158	0.06	22.28	compression
G7	17.4	1.56	18657	853	0.05	32.33	compression
G8	17.68	1.75	16438	963	0.06	36.18	compression

ISSN: 2277-3754
ISO 9001:2008 Certified
International Journal of Engineering and Innovative Technology (IJEIT)
Volume 5, Issue 2, August 2015

Load-tendon stress relations are drawn in Fig. 7, which shows that CFRP tendon capacity has not fully used in specimens C5 and C6 (waste of prestressing), but fully used in C7 and C8 specimens. For AFRP and GFRP specimens tendons capacity has not fully utilized.

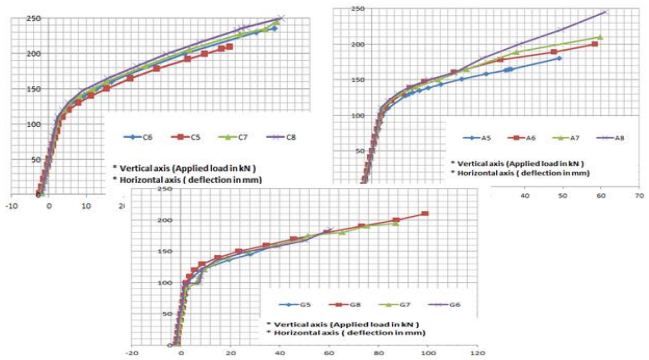

Fig. 5: Load-deflection relations

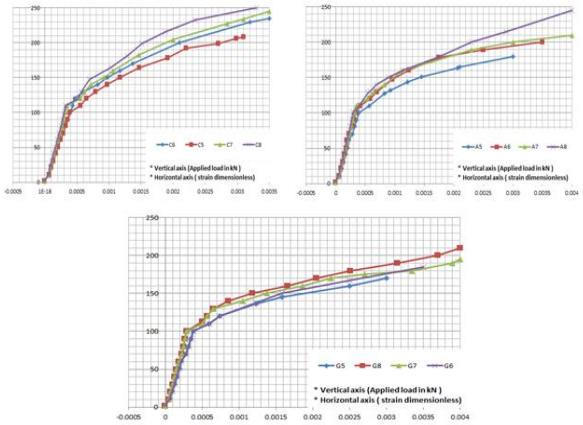

Fig: 6 Load-concrete strain relations

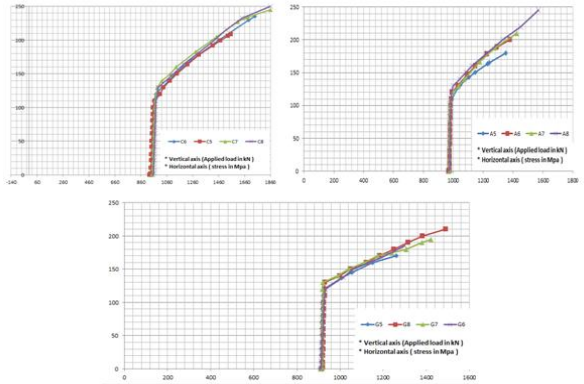

Fig. 7: Load-tendon stress relations

C. *Effect of prestressing Level (P)*

To study the effect of prestress level of on flexural response, nine specimens of CFRP, AFRP, and GFRP strands, with prestress levels, 70%, 60%, and 50% were investigated. Concrete strength f_{cu}=*35 MPa* and tendon eccentricity *e=50 mm*, while prestress reinforcement ratio ρ is chosen 0.63% for CFRP, and 0.49% for AFRP, and GFRP to obtain compression failure. Results are listed in Table 8, Table 9, and load- deflection relations are plotted in Fig. 8.

For the specimens (C1, C9, C10, A2, A9, A10, G2, G9, G10), the failure mode for these specimens was brittle failure, differs at location with changing prestressing force. Failure location is changed from compression at concrete to tension at tendons by increasing prestressing force. The use of high prestressing force (70%) leads to significant improvement in flexural capacity with low ductility and deformability. The use of prestressing force (50%-60%) leads to significant improvement in ductility, deformability and flexural capacity.

The prestressing levels in FRP cables have significantly affected the load-deflection responses of the prestressed beams. From the results it is observed that the ultimate deformation capacity increases for the lower prestressing level.

On the other hand the ultimate load capacity slightly increases by increasing prestressing level. The energy absorption index of the CFRP-prestressed beam with P =50 %is found to be higher than that of CFRP-prestressed beam with P = 60 % by about 25% and higher than that of CFRP-prestressed beam with P = 70% by about 45%. The ductility index of the CFRP-prestressed beam with P =50% is found to be higher than that of CFRP-prestressed beam with P = 60 %by about 20% and higher than that of CFRP-prestressed beam with P = 70 % by about 50%.

The energy absorption index of the AFRP-prestressed beam with P =50% is found to be higher than that of AFRP-prestressed beam with P = 60% by about 20% and higher than that of AFRP-prestressed beam with P % = 70 by about 40%. The ductility index of the AFRP-prestressed beam with P =50% is found to be higher than that of AFRP-prestressed beam with P = 60 % by about 14% and higher than that of CFRP-prestressed beam with P = 70% by about 34%.The energy absorption index of the GFRP-prestressed beam with P =50% is found to be higher than that of GFRP-prestressed beam with P = 60% by about 10% and higher than that of GFRP-prestressed beam with P = 70% by about 50%. The ductility index of the GFRP-prestressed beam with P % =50 is found to be the same ductility of GFRP-prestressed beam with P = 60% and higher than that of CFRP-prestressed beam with P = 70 % by about 37%.

It may be seen that μ_Δ and E.A.I decreases with an increase in level of prestressing for all types of fibers.

Table 8 Loads-Deflections values at variable P%

Speci.	P %	P_{cr} kN	Δ_{cr} mm	P_{el} kN	Δ_{el} mm	P_u kN	Δ_u mm
C1	70	128	3.7	145	6	233	34.6
C9	60	114	3.5	125	5.2	220	45.9
C10	50	108	2.4	120	5.2	215	58
A2	70	116	3.6	130	6	190	54.5

ISSN: 2277-3754
ISO 9001:2008 Certified
International Journal of Engineering and Innovative Technology (IJEIT)
Volume 5, Issue 2, August 2015

A9	60	103	3	110	4.7	170	55.6
A10	50	94	3.4	102	4.6	160	63.2
G2	70	125	4	135	6	170	39
G9	60	103	3.3	112	4.7	160	48.9
G10	50	92	3.5	100	5.3	150	54.7

Table 9 Computed data at variable P%

Speci.	μ_Δ	Ω	K_i	K_p	K_p/K_i	E.A.I	Failure mode
C1	5.76	1.61	16111	3081	0.19	9.27	comp.
C9	8.83	1.76	16026	2334	0.15	15.4	comp.
C10	11.15	1.79	15789	1799	0.11	20.4	comp.
A2	9.08	1.46	14943	1237	0.08	14.72	comp.
A9	11.83	1.55	15714	1178	0.075	19.5	comp.
A10	13.74	1.58	15379	998	0.065	23.87	comp.
G2	6.5	1.26	15698	1060	0.068	9.67	comp.
G9	10.4	1.43	15929	1097	0.069	16.38	comp.
G10	10.32	1.5	13889	1012	0.073	18.15	comp.

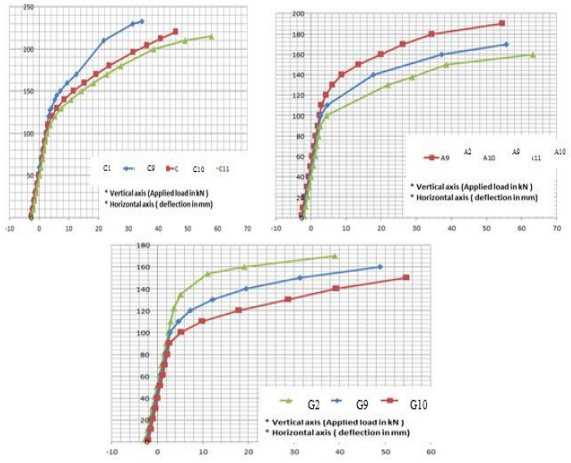

Fig. 8: Load-deflection

The Load-Concrete Strains are shown in Fig. (9), it is observed that concrete resistance has fully utilized at all specimens for all types of fiber tendons. The Load - Tendons Stresses are also shown in Fig. (10), for carbon tendons, it is observed that tendon capacity had not fully consumed at all specimens so we can say all of them are not economically viable. For aramid tendons it is observed that tendon capacity had not fully utilized at all specimens. The most economic one is A2 which utilized about 81% from tendon capacity. For glass tendons it is observed that tendon capacity had not fully utilized at all specimens. The most economic one is G2 which utilized about 83% from tendon capacity.

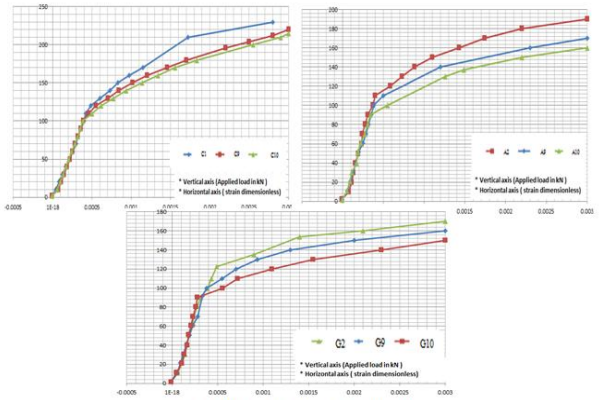

Figure 9: Load-Concrete Strains

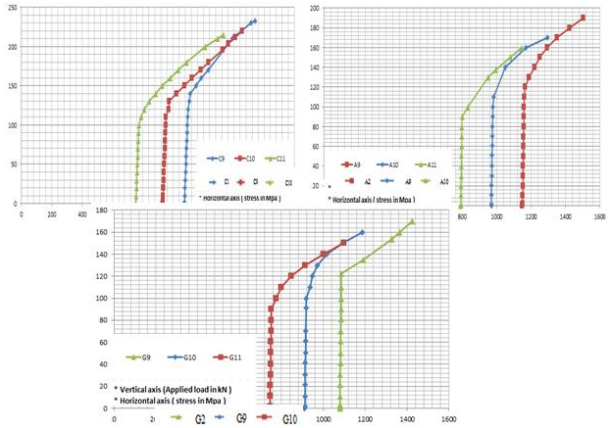

Figure 10: Load-Tendon Stresses

VI. CONCLUSIONS

1- The flexural prestressing reinforcement ratio **ρ**, concrete compressive strength f_{cu}, and initial prestressing force P% affects the flexural behavior and failure modes of the concrete beam models.

2- The increase of flexural prestressing reinforcement ratio **ρ** for all types of FRP tendons increases load carrying capacity, due to vital role of the tension prestressing reinforcement in reducing crack width and prevent crack from developing at low load levels.

3- For CFRP, and AFRP tendons, the optimum flexural behavior attained at **ρ** =0.494 % for best characteristics in both strength and ductility, while for GFRP tendons, the high strength and ductility achieved at ρ = 0.633%.

4- For all types of fiber tendons, as the concrete compressive strength increased, the load-carrying capacity increased.

5- For CFRP tendons to achieve high strength and ductility, the concrete compressive strength (f_{cu}) equal 45 MPa. While for AFRP, and GFRP tendons, the optimum characteristics in both strength and ductility achieved at f_{cu} equal (50-60) MPa.

6- For CFRP, AFRP and GFRP tendons the optimum flexural behavior attained at P = (50%-60%) with significant improvements in ductility.

7- Design of tension failure assumption in not recommended for all types of FRP tendons.

ISSN: 2277-3754
ISO 9001:2008 Certified
International Journal of Engineering and Innovative Technology (IJEIT)
Volume 5, Issue 2, August 2015

8- Design of balanced failure assumption is recommended only for CFRP tendons at concrete compressive strength equal 45 MPa with level of prestressing force (P) ranging from (50-60)%.

9- Design of compression failure is recommended for all types of FRP tendons at ρ=0.56 and P=60%. The preferable value of f_{cu} for CFRP tendons equals 45 MPa, and 60 MPa for AFRP and GFRP tendons.

10- Design for resisting dynamic loads and extreme loading conditions such as earthquakes is preferred for all types of tendons at f_{cu} equal 35 MPa, but the preferable values of P and ρ respectively, for CFRP tendons equal 50% and 0.633, for AFRP tendons equal 70 and 0.294 and for GFRP tendons equal 70% and 0.19.

REFERENCES

[1] Adorjan Borosnyol, "Serviceability of CFRP Prestressed Concrete Beam," PhD Thesis Budapest University of Technology and Economics", 2002.

[2] Amir Z.Fam, "Carbon Fibre Reinforced Plastic Prestressing and Shear Reinforcements for Concrete Highway Bridges," presented to the University of Manitoba in Master of Science,", 1995.

[3] Yonekura, A., Tazawa, E., and Nakayama, H., "Flexural and Shear Behavior of Prestressed Concrete Beams," ACI special publications; 138; 525-548, 1993.

[4] Tan K. H., Farooq, Abdullah-Al, and Ng, Chee-Khoon, "Behavior of Simple Span Reinforced Concrete Beams Locally Strengthened with External Tendons," ACI Structural Journal, Vol. 98, No. 2. 2001.

[5] Rizkalla, S. and Labossiere, P., "Structural Engineering with FRP,"in Canada: Planning for a New Generation of Infrastructure Concrete International, Vol. 20, Issue 6, pp. 35-38. June 1999.

[6] Mutsuyoshi H., and Machida, A., "Behavior of Prestressed Concrete Beams Using FRP as External Cable," Volume 138, pp 401-418, publication date 9/1/1 993.

[7] Maissen, A., and De Semet, C. A. M., "Comparison of Concrete Beams Prestressed with Carbon Fiber-reinforced Plastic and Steel Strands," International RILEM, Belgium, pp430-439, 1995.

[8] Kato,T., and Hayashida, N., "Flexural Characteristics of Prestressed Concrete Beams with CFRP Tendons," ACI Structural Journal, Vol. 138, Issue 1, pp. 419-440, 1993.

[9] Rizkalla, S., and Tadros, G., "FRP for Prestressing of Concrete Bridges in Canada," ACI Structural Journal, Vol. 94, Issue 1, pp. 77-86, January/February 1997.

[10] Nabil F. Grace, "Experimental Study and Analysis of a Full-Scale CFRP/CFCC Double-Tee Bridge Beam," PCI Journal August 2003.

[11] Nabil F. Grace, "Flexural behavior of precast concrete box beams post tensioned with unbounded carbon fiber composite cables," PCI JOURNAL summer 2008.

[12] J.W. Schmidt & B. Täljsten, "FRP tendon anchorage in post-tensioned concrete structures," Concrete Repair, Rehabilitation and Retrofitting II –Francis Group, London, ISBN 978-0-415-46850-3, 2009.

[13] Nabil F. Grace, "Transverse diaphragms and un bonded CFRP post tensioning in box-beam bridges," PCI Journal, 55:109-122, 3-2010.

[14] CSA, " Design and construction of building components with fiber-reinforced polymers," CSA standard CAN/CSA S806-02 " Canadian Standards Association, Rexdale, Ont. 2002.

[15] Martin NOËL, "Effect of post-tensioned CFRP tendons on the flexural performance of GFRP reinforced slab bridges," PhD Thesis University of Waterloo, 2007.

[16] Nolan G. Domenico, "Bond properties of CFCC prestressing strands In pretension concrete beams," Master Thesis University of Monitoba 'Winnipeg, Monitoba, 1995.

AUTHOR BIOGRAPHY

First Author Mohamed Husain, Professor Structural Engineering Department, Faculty of Engineering, Zagazig University, Zagazig, EGYPT.

Second Author Khaled Fawzy, Assistant Professor Structural Engineering Department Faculty of Engineering, Zagazig University, Zagazig, EGYPT

Third Author research engineer.